The Dynamic Impact of CpG Methylation in DNA†

Karen B. Geahigan,‡ Gary A. Meints, Mary E. Hatcher,§ John Orban,|| and Gary P. Drobny*

Departments of Chemistry and Physics, University of Washington, Seattle, WA 98195

Received July 28, 1999; Revised Manuscript Received December 6, 1999

ABSTRACT: Solid-state deuterium NMR is used to investigate perturbations of the local, internal dynamics in the *Eco*RI restriction binding site, -GAATTC- induced by cytidine methylation. Methylation of the cytidine base in this sequence is known to suppress hydrolysis by the *Eco*RI restriction enzyme. Previous solid-state deuterium NMR studies have detected large amplitude motions of the phosphate−sugar backbone at the AT−CG junction of the unmethylated DNA sequence. This study shows that methylation of the cytidine base in a CpG dinucleotide reduces the amplitudes of motions of the phosphate−sugar backbone. These observations suggest a direct link between suppression of the amplitudes of localized, internal motions of the sugar−phosphate backbone of the DNA and inhibition of restriction enzyme cleavage.

Methylation is a chemical modification of DNA that is considered vital for normal cellular development. In prokaryotic cells, DNA methylation is involved primarily in restriction-modification systems that serve to prevent phage infection. Prokaryotic DNA is methylated by three distinct types of methyltransferases, the simplest being the type II methylases that are cognate to the well known restriction endonucleases (*1*). Type II methylases attach methyl groups to the C5 or N4 positions of 2′-deoxycytidine or the N6 position of 2′-deoxyadenosine (Figure 1). In eukaryotic systems, DNA methylases preferentially act on hemimethylated DNA where the recognition sequence is simply CpG in most animals. S-Adenosyl-methionine donates the methyl group for the transmethylation reaction, which produces 5-methylcytosine (5-mC) (Figure 1A) (*2*).

There are significant consequences to the presence of methylated CpG dinucleotides. Many transcription factors no longer efficiently bind DNA when their recognition sites are methylated (*2*, *3*), and gene silencing in eukaryotes is thought to result from methylation either directly, by interfering with the interaction of a transcription factor with its recognition site, or indirectly, by attracting proteins that have a high affinity for methylated DNA. For example, methylation-induced structural and/or dynamical changes within a triplet of CpG dinucleotides have been shown to directly contribute to translational positioning of nucleosomes by affecting binding of the histone octamer (*4*). Methylated CpG dinucleotides are also sites for a high percentage of point mutations (*5*), and abnormal methylation patterns in DNA have been linked to various cancers and to genetic disorders such as fragile X syndrome (*2*, *3*, *6*).

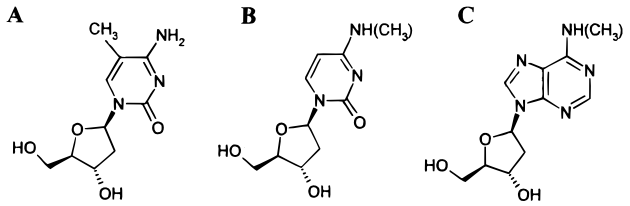

FIGURE 1: Structures of (A) C5-methyl-2′-deoxycytidine, (B) N4-methyl-2′-deoxycytidine, and (C) N6-methyl-2′-deoxyadenosine.

Despite abundant evidence supporting the biological importance of CpG methylation, experimental data do not as yet provide a clear picture of the relationship between the functional impact of DNA methylation and the structure of methylated DNA. Although cytosine methylation increases the thermal stability of the DNA and gel electrophoresis assays show that CpG methylation alters DNA bending (*7*), neither X-ray diffraction nor solution NMR studies of singly CpG-methylated DNA oligomers indicate substantial structural alteration (*8*−*10*).

There is, however, abundant evidence that deformation of the DNA duplex structure is an important component of many DNA−protein interactions (*11*). In addition, deformability of the DNA helix may be manifested by increased amplitudes of localized motions in the native DNA sequence cleaving (*12*). If localized motions of the DNA duplex impart flexibility to the structure that in turn enables optimization of interactions with proteins, then chemical modifications that affect protein−DNA interactions may do so by perturbing amplitudes and possibly the rates of these localized motions. Thus, the impact of methylation on DNA may be partially dynamic, rather than strictly structural in nature.

To thoroughly assess the impact of CpG methylation on internal DNA dynamics and in particular to determine the degree to which cytosine methylation perturbs internal

† This research was supported by NIH grant RO1 GM58914-01. Karen Geahigan and Gary Meints acknowledge support from NIH Training Grant GM32681.

* To whom correspondence should be addressed. Department of Chemistry, University of Washington, Box 351700, Seattle, Washington 98195. Telephone: (206)685-2052. E-mail: drobny@macmail.chem.washington.edu/ Fax: (206) 685-8665.

‡ Present address: 270-2N-15, 3M Center, St. Paul, MN 55144.

§ Present address: WM Keck Science Center, The Claremont Colleges, 925 North Mills Avenue, Claremont, CA 91711.

|| Present address: Center for Advanced Research in Biotechnology, University of Maryland, Biotechnology Institute, Rockville, MD 20850.

[1] Abbreviations: NMR, nuclear magnetic resonance; DNA, deoxyribonucleic acid.

10.1021/bi9917636 CCC: $19.00
Published on Web 03/30/2000

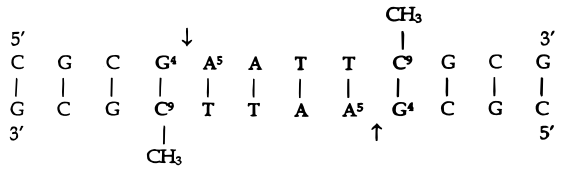

FIGURE 2: DNA sequence containing the *Eco*RI restriction site -GAATTC-, with C5-methyl-2′-deoxycytidine at the C_9 position. The binding site is in bold, with the cleavage sites indicated by the arrows.

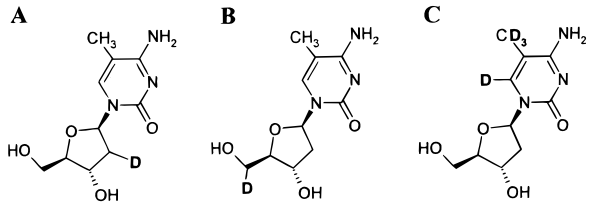

FIGURE 3: Location of deuterium labels in this study. (A) [2″-^{2}H]-5-methyl-2′-deoxycytidine. (B) [5′/5″-^{2}H]-5-methyl-2′-deoxycytidine (C) [d_6, methyl-^{2}H]-5-methyl-2′-deoxycytidine.

motions of the DNA helix in the neighborhood of a CpG methylation site, we have used solid-state deuterium (^{2}H) NMR line shape and spin−lattice relaxation measurements to monitor the perturbation on local base, sugar ring, and backbone dynamics resulting from introduction of 5-methyl-2′-deoxycytidine at a CpG dinucleotide in a DNA oligomer by specifically deuterating four separate sites in the cytidine. Specifically, we have chosen to methylate the cytidine nucleotide (shown as the underlined C, and hereafter referred to as C_9) in the DNA dodecamer, [d(CGCGAATT*C*GCG)]$_2$, which contains the binding site d(GAATTC) for the restriction endonuclease *Eco*RI. The C_9pG_{10} dinucleotide is located directly on a cross strand from the *Eco*RI restriction enzyme cleavage site (Figure 2).

Although not a target site for a methyltransferase, the C_9-pG_{10} dinucleotide in the dodecamer [d(CGCGAATTCGCG)]$_2$, nevertheless, serves as a useful model system for studying the dynamic impact of CpG methylation. The target of the bacterial methylase is the adenine N6 in the AATT moiety, but steady-state kinetic measurements indicate that methylation at the C5 position on C_9 suppresses cleavage of the phosphodiester backbone by *Eco*RI to an equivalent extent (*1*). Despite the marked impact that C_9 methylation exerts on the rate of restriction enzyme cleavage, X-ray crystallography data show little structural alteration as a result of methylating this position (*8*). Although contacts between residues of the *Eco*RI restriction enzyme and the phosphodiester backbone at the C_9pG_{10} step are observed in the crystal structure of the protein−DNA complex (*13*), no sequence-specific contacts between the *Eco*RI restriction enzyme and the base of C_9 have been reported.

The functional impact of CpG methylation in this particular system might be more fully understood in terms of the influence that C_9 base methylation exerts on the local internal dynamics, and thus the local flexibility of this DNA sequence. Solid-state deuterium NMR studies indicate the presence of large amplitude motions of the phosphodiester backbone at C_9 (*14*). Notably, this mobile nucleotide is located at the AT−GC junction, which is marked by a 18 degree bend in the crystal structure (*15*) and which has been hypothesized to be a deformable hinge that can be bent by local forces (*16*). This region of the DNA dodecamer is also markedly kinked in the complex with the restriction enzyme (*13*). Specific questions that we address here are: does 5-methylation of C_9, which diminishes the rate of restriction enzyme catalyzed hydrolysis of DNA, also perturb the amplitudes and/or rates of localized dynamics near the methylation site, and can any observed dynamical changes be reconciled with observed functional changes resulting from methylation?

MATERIALS AND METHODS

Chemical Synthesis of Selectively Deuterated, Methylated DNA. To investigate the degree to which methylation perturbs the dynamics of the furanose ring, the backbone, and the base of the methylated C_9 nucleotide, selectively deuterated nucleosides were synthesized (Figure 3A, B, and C) and incorporated into the DNA dodecamer, using phosphoramidite chemistry. Deuterated DNA oligonucleotides were synthesized as follows. [2″-^{2}H]-2′-deoxythymindine was prepared by the method of Robins et al., with some minor modifications to the solvent systems (*17*). [5′/5″-^{2}H]-2′-deoxythymidine was prepared by the method of Orban and Reid (*18*). [6-methyl-$^2H_4$]-2′-deoxythymidine was prepared by enzymatically glycosylating [d_6, methyl-$^2H_4$]-thymine, using 2′-deoxyadenosine as the pentosyl donor (*19*). Deuterated 2′-deoxythymidine (dT) nucleosides were converted to 5′-O-(DMT)-2′-dT-3′-CED-phosphoramidites as described previously and converted to N4-triazole derivatives using the procedure of Cowart et al. (*20*). N4-triazole phosphoramidites were incorporated at the 9 position of the growing DNA oligonucleotide sequence using an ABI Model 394 automated DNA/RNA synthesizer. Deprotection of the DNA in concentrated ammonia (2 days, 55 °C) converted the N4-protected thymidine derivative to the 5-methyl-2′-deoxycytidine nucleotide. Oligonucleotides were purified as described previously, salted (10% NaCl by weight), packed into a 5 mm solid-state NMR Kel-F rotor, and hydrated by vapor diffusion in a humidity chamber containing saturated $NaClO_4$ in ^{2}H-depleted water (75% relative humidity at 20 °C) (*21*). Water content was quantified gravimetrically by the parameter *W* (number of water molecules per nucleotide) and is accurate to ±2 waters per nucleotide.

Solid-State NMR Spectroscopy. All ^{2}H NMR experiments were performed on a home-built NMR spectrometer (11.75 T, deuterium Larmor frequency of 76.776 MHz.). A quadrupolar echo pulse sequence with an eight-step phase cycling scheme was implemented with a delay of 40 μs between 90° pulses (typically, 1.8−2.5 μs in duration) and a dwell time of 200 ns during acquisition. Data acquisition was initiated prior to the echo maximum. The time domain data were left-shifted and apodized with 1000−4000 Hz. Lorentzian line broadening prior to Fourier transformation. Spin−lattice relaxation times were determined using an inversion recovery pulse sequence, which incorporated a 180° composite pulse to ensure broadband excitation (*22*). All lineshape and Zeeman spin−lattice relaxation data were collected at room temperature. To obtain powder-averaged Zeeman spin−lattice relaxation times $<T_{1Z}>$, the integrated intensity of the powder spectrum was monitored as a function of recovery time and analyzed using a nonlinear least-squares

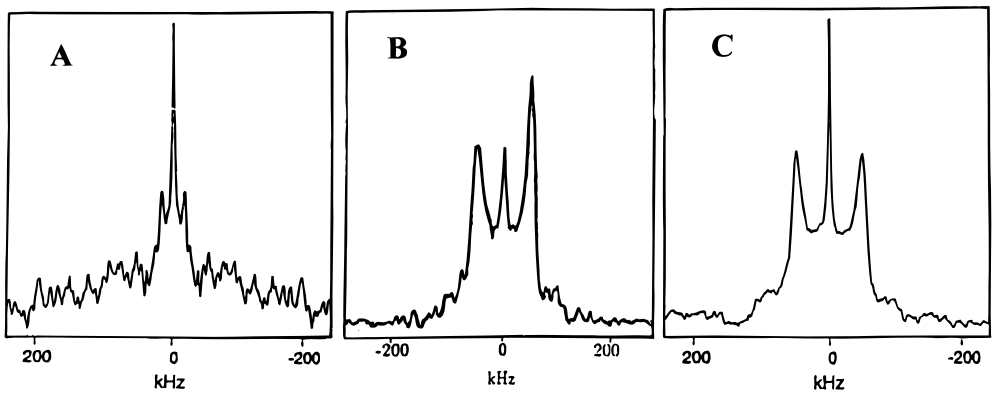

FIGURE 4: (A) Solid-state ^{2}H quadrupolar echo line-shape of [5′/5″-^{2}H]-C_9 at $W = 10.1$. The signal-to-noise of this sample is lower due to smaller sample size and incomplete deuteration. (B) Solid-state ^{2}H quadrupolar echo line-shape of [5′/5″-^{2}H]-T_7 at $W = 10.5$ (C) Solid-state ^{2}H quadrupolar echo line-shape of [5′/5″-^{2}H]-$^{5Me}C_9$. Central isotropic component is due to residual HDO in hydrated oligonucleotide samples.

Table 1: Spin−Lattice Relaxation Times for C_9[a]

position of deuterium label	methylated?	spin−lattice relaxation time (seconds)	hydration level (waters/nucleotide)
C5′/C5″	no	0.030	10.1 (± 2)
C5′/C5″	yes	0.055	13.1 (± 2)
C2″	no	0.020	12.3 (± 2)
C2″	yes	0.017	9.5 (± 2)
C5,C6	no	0.1	10.1 (± 2)
C6	yes	0.15	12.1 (± 2)

[a] Spin−lattice relaxation times of C_9 with the backbone, furanose ring, and base deuterium labels for both methylated and unmethylated samples.

fitting routine (*23*). Dynamically averaged deuterium line-shapes were simulated using MXET1 (*24*).

EXPERIMENTAL RESULTS

Deuterium Line-Shape and Relaxation Data for 5′/5″ Deuterons. Quadrupolar echo line-shapes and spin−lattice relaxation data were obtained for the [d_6, methyl-$^2H_4$], [2″-^{2}H]- and [5′/5″-^{2}H]-$^{5Me}C_9$ labeled DNA dodecamers. The impact that cytosine base methylation has on the dynamics of the 5′-methylene deuterons of C_9 is shown in Figure 4. The quadrupolar echo spectrum obtained from 85 mg [5′/5″-^{2}H]-$^{5Me}C_9$-DNA at $W = 13.1$ has the form of a Pake doublet powder pattern with an effective quadrupolar coupling constant of $QCC_{eff} = 148$ kHz (Figure 4C). Similar studies of [5′/5″-^{2}H]-$^{5Me}C_9$-DNA at $W = 15.2$ and 16.5 show only small reductions of the *QCC* to approximately 145 and 143 kHz, respectively (data not shown). From a comparison of Figure 4 parts A, B, and C, it is clear that methylation of the base of C_9 has resulted in a marked perturbation of the 5′-methylene group line-shape of C_9, implying a significant reduction in the amplitude of the local dynamics of the phosphodiester backbone displacement.

Further insight into the internal dynamics of the 5′-methylene at C_9 and the impact exerted by cytosine methylation may be obtained from deuterium spin−lattice relaxation data, shown in Table 1. Inversion recovery data for the [5′/5″-^{2}H]-$^{5Me}C_9$ dodecamer sample at $W = 13.1$ was fit to a single-exponential, which gave a spin−lattice relaxation time, $<T_{1Z}>$, of 0.055 s. This differs from unmethylated C_9, which yielded a $<T_{1Z}>$ of only 0.030 s for the 5′/5″ deuterons of C_9 at $W = 10.1$. On the other hand, relaxation data for the [5′/5″-^{2}H]-$^{5Me}C_9$ dodecamer are similar to that reported by Alam et al. for the 5′-methylene deuterated T_7/T_8 dodecamer (0.059 s at $W = 10.5$) (*26*). Therefore, spin−lattice relaxation data for the [5′/5″-^{2}H]-$^{5Me}C_9$ analogue again reveals that methylation of the C_9 nucleotide effectively perturbs the mobility of the 5′-methylene group as shown by a near doubling of the spin−lattice relaxation time $<T_{1Z}>$ in methylated vs unmethylated DNA at $W = 10-13$. In fact, even at hydration levels as high as $W = 16.5$, $<T_{1Z}>$ for the [5′/5″-^{2}H]-$^{5Me}C_9$ dodecamer decreases to only 0.044 s, which is still significantly longer than the $<T_{1Z}>$ value of 0.03 s observed for the unmethylated analogue at $W = 10.1$.

Deuterium Line-Shape and Relaxation Data for the 2″ Deuteron. The effect that C_9 methylation has on furanose ring dynamics is shown in Figure 5, parts A and B, which are deuterium powder line-shapes for the [2″-^{2}H]-$^{5Me}C_9$- and [2″-^{2}H]-C_9-DNA samples at $W = 9.5$ and 10, respectively. The spectrum for the unmethylated [2″-^{2}H]-C_9-DNA dodecamer displays a line-shape characteristic of intermediate motional averaging and has been simulated as a two site jump (equal a priori site probabilities, half amplitude = 38°) of the C2′−D2″ bond at a rate on the order of 10^7 Hz (*14*). Inspection of the line-shape for 54 mg of the [2″-^{2}H]-$^{5Me}C_9$ analogue reveals that the 2″ deuteron is still relatively mobile, with spectral distortions characteristic of a C−D bond that is undergoing conformational exchange at intermediate rates with a significant amplitude.

Although the line-shape data in Figure 5 data indicate that methylation has less effect on furanose mobility than on backbone mobility at C_9, the $W = 9.5-10$ line-shapes for the furanose-deuterated methylated and unmethylated DNA's differ in several details, notably at the spectral maxima where the methylated analogue displays a distinct "triplet" structure. These features, located at ±16, 32, and 50 kHz, are well above the level of the spectral noise and do not appear in the unmethylated sample. Spectral differences between the methylated and unmethylated samples persist to higher hydration levels ($W = 12-14$) as shown in Figure 6 parts A and B. Relaxation data show a very modest change upon methylation (Table 1). The inversion recovery experiment for the [2″-^{2}H]-$^{5Me}C_9$ dodecanucleotide sample at $W = 9.5$ yielded a spin−lattice relaxation time $<T_{1Z}>$ of 0.017 s. In comparison, $<T_{1Z}>$ for the [2″-^{2}H]-C_9-DNA dodecanucleotide at $W = 12.3$ was approximately 0.020 s (*14*).

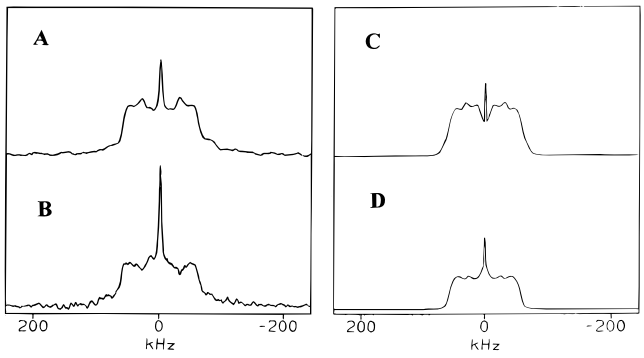

FIGURE 5: (A) Solid-state ^{2}H quadrupolar echo line-shape of [2″-^{2}H]-5MeC$_9$ at $W = 9.1$. (B) Solid-state ^{2}H quadrupolar echo line-shape of [2″-^{2}H]-C$_9$ at $W = 10-11$. (C) Best fit simulation of (A), using single axis Brownian diffusion model described in text. Barrier heights are 5 k_BT, with half-angle amplitude of 34° and rate constant of $k = 7.5 \times 10^7$ Hz. (D) Best fit simulation of (B), using single axis Brownian diffusion model described in text. Barrier heights are 5 k_BT, with half-angle amplitude of 38° and rate constant of $k = 7.5 \times 10^7$ Hz.

Deuterium Line-Shape and Relaxation Data for Deuteron 6. Figure 7A shows the deuterium NMR line-shapes obtained for the [d_6, methyl-^{2}H$_4$]-^{5Me}C$_9$ dodecanucleotide at $W = 12.1$. The inner Pake doublet, with a QCC_{eff} of 50 kHz corresponds to the CD$_3$ group of the 5-methylcytosine where the spectral narrowing results from the rapid rotation of the methyl group. The less intense outer Pake doublet is due to the deuteron bonded to the C6 carbon of C$_9$ (i.e., the D6 deuteron). Vertical expansion of this spectrum, shown in Figure 7B, serves to display more clearly the NMR signal arising from the D6 deuteron. Although the spectrum of the CD$_3$ group obscures the central portion of the D6 Pake doublet, the perpendicular edges (i.e., "horns") of the D6 deuteron's Pake doublet are clearly resolved. Therefore, the effective quadrupole coupling constant QCC_{eff} for D6 can be measured from the horn-to-horn splitting and from the relationship $QCC_{eff} = 4\delta/3$ where δ is the horn-to-horn splitting. By this method, the QCC_{eff} for the D6 deuteron in methylated C$_9$ is found to be 155 kHz at $W = 12.1$. The D6 line-shape has a small effective asymmetry parameter of $\eta_{eff} = 0.06$ at $W = 12.1$.

Additionally, the spin−lattice relaxation times for the D6 deuterons in methylated have been obtained (Table 1). For the [5,6-^{2}H]-C$_9$ at $W = 10.1$, $<T_{1Z}> = 0.1$ s, which is typical for a base deuteron at this hydration level *(14)*.

DISCUSSION

The solid-state deuterium line-shapes and relaxation data, reported in the preceding section, may be compared to previously published data for the unmethylated analogues (*14*) (*25*), also obtained at 76.776 MHz. These comparisons of the line-shapes and relaxation data show that methylation of the cytosine heterocycle perturbs the local mobility (amplitude and/or rate) of the backbone, the furanose ring, and the base to differing extents. To obtain a clear physical picture of the dynamic impact of DNA methylation, the changes in dynamic amplitude and rate of localized motions of the phosphodiester backbone, furanose ring, and cytosine base introduced by methylation were simulated using several dynamic models.

Analysis of Backbone Motions. Solid-state deuterium line-shape data obtained for the unmethylated [5′/5″-^{2}H]-C$_9$-DNA at $W = 10.5$ (Figure 4A) reveal that the preaveraged or effective quadrupolar coupling constant (QCC_{eff}) does not exceed 60 kHz (*14*). This represents a dramatic reduction of the quadrupolar coupling constant from its static value (QCC_{static}) of approximately 164 kHz. This reduction is attributable to a fast motion ($t_c \ll 10^{-7}$ s) that modulates the orientation of the C5′-D5′/5″ bond through a large angle. Other solid-state deuterium NMR line-shape studies show that the phosphodiester backbone of the DNA dodecamer is not uniformly flexible. In contrast to data gathered for the 5′-methylene group of C$_9$, solid-state deuterium NMR line-shape and relaxation data acquired for the 5′/5″ deuterons of the nearby T$_7$ and T$_8$ nucleotides in a DNA dodecamer of the same sequence (see Figure 4B) indicate more modest averaging of the 5′/5″ deuterium line-shape, with the QCC_{eff} equal to 150 kHz at $W = 11.9$ and 143 kHz at $W = 16.3$ (*26*). When the C$_9$ nucleotide is methylated, the solid-state deuterium NMR spectrum of 5′/5″ deuterons of this nucleotide now resembles the spectral line shapes observed at T$_7$ and T$_8$ in the same DNA sequence (*26*). The more modest reductions of the *QCC*'s of the 5′/5″ deuterons of the T$_7$ and T$_8$ nucleotides could not be simulated as an exchange between all three rotational isomers of the C4′-C5′ bond at hydration levels typical of B-form DNA. Rather, these data indicate that at $W = 11.9$ the C5′-D5′/5″ bonds of T$_7$ and T$_8$ librate about a single bond conformer with a root-mean-square displacement of less than 20 degrees. The QCC_{eff} reported for methylated C$_9$ indicates that, like T$_7$ and T$_8$, the ^{5Me}C$_9$ C5′-D5′/5″ bond librates about a bond with similar magnitude of displacement.

Analysis of Furanose Ring Motions. Furanose ring motions in DNA are frequently modeled as interconversions between discrete pseudorotational conformers (*27*). The simplest models portray furanose dynamics as an exchange between two conformers (*14*, *28*−*30*) (e.g., C2′-endo and C3′-endo), although recent experimental analyses of proton scalar coupling constants in DNA assume exchange between a greater number of conformers (*31*). Although activated exchange between discrete conformations of the furanose ring is a good approximation of internal molecular motions when kinetic barriers exceed 10 k_BT (5.8 kcal/mol), theoretical estimates of the barrier to exchange between C2′-endo and C3′-endo range from only 0.5 kcal/mol (*29*), a remarkably low barrier indicating virtually free pseudorotation, to about 2−5 kcal/mol (*32*). Therefore, discrete site exchange may be a poor approximation for furanose ring motions in DNA.

A more realistic model of furanose ring motion assumes the C−D bonds undergo angular Brownian diffusion in a potential U. If we assume the angular diffusion of the C2′−D2″ is one-dimensional (see Figure 8), then we can describe the potential U as a function of a single angle ϕ. In this case the time-dependent probability distribution function $P(\phi,t)$ for the C2′−D″ bond satisfies the Smoluchowski equation:

$$\frac{\partial P(\phi,t)}{\partial t} = R(\phi)P(\phi,t) \qquad (1)$$

where the operator $R(\phi)$ is given by:

$$R(\phi) = D\left[\frac{\partial^2}{\partial \phi^2} + \frac{1}{kT}U'(\phi)\frac{\partial}{\partial \phi} + \frac{1}{kT}U''(\phi)\right] \qquad (2)$$

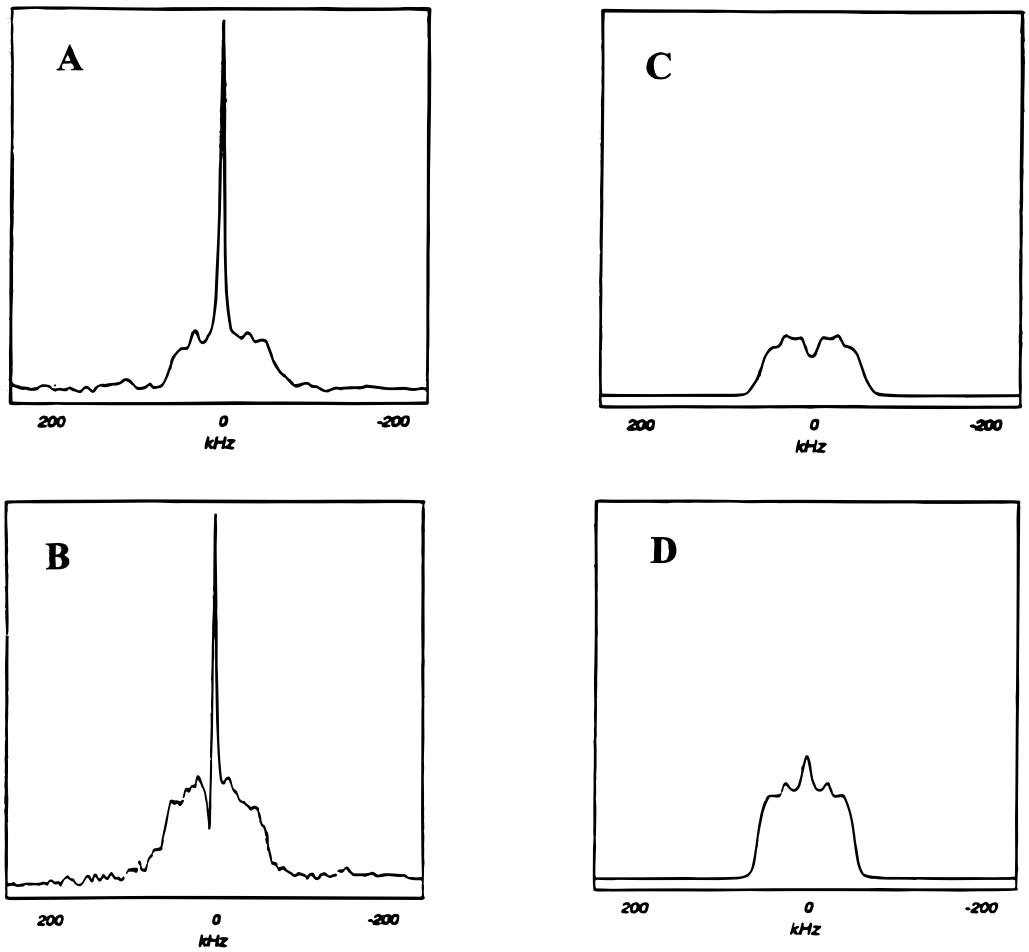

FIGURE 6: (A) Solid-state ^{2}H quadrupolar echo line-shape of [2″-^{2}H]-5MeC$_9$ at $W = 13.8$ (B) Solid-state ^{2}H quadrupolar echo line-shape of [2″-^{2}H]-C$_9$ at $W = 12-13$. (C) Best fit simulation of (A), using single axis Brownian diffusion model described in text. Barrier heights are 5 k_BT, with half-angle amplitude of 34° and rate constant of $k = 10^8$ Hz. (D) Best fit simulation of (B), using single axis Brownian diffusion model described in text. Barrier heights are 5 k_BT, with half-angle amplitude of 38° and rate constant of $k = 10^8$ Hz.

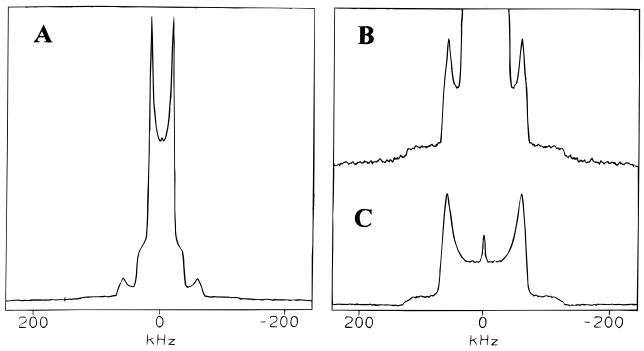

FIGURE 7: (A) Solid-state ^{2}H quadrupolar echo line-shape of [d_6, methyl-^{2}H]-5-methyl-C$_9$ at $W = 12.1$. (B) Expansion of (A), to better show the signal from the D6 deuteron. (C) Solid-state ^{2}H quadrupolar echo line-shape of [5,6-^{2}H]-C$_9$ at $W = 10-11$.

D is the ϕ-independent diffusion coefficient describing the rate of motion of the C−D bond in the potential $U(\phi)$. A finite difference approximation to $R(\phi)$ has been developed by Nadler and Shulten (*33*). This discretized treatment of diffusion in a potential has been used to quantify the influence of atomic motions on the Mossbauer line shape of ^{57}Fe in proteins (*34*), and the effect of molecular motions on the deuterium NMR spectra of lipids (*35*). A similar formulation has been used by Edholm and Blomberg to quantify solution NMR relaxation times of ^{13}C spins in protein side-chains (*36*) and by Torchia and Szabo to calculate deuterium NMR relaxation times of methyl groups in solids (*37*). For the purpose of describing furanose ring dynamics in DNA, we assume $R(\phi)$ can be approximated by a kinetic matrix R_{ij} where matrix elements of R are defined as:

$$R_{ij} = \frac{1}{\tau_c} \frac{P_i}{P_{i\pm1}} \; j = i \pm 1 \qquad (3)$$

$$R_{ij} = -(R_{i,i-1} + R_{i,i+1}) \; j = i$$

$$R_{ij} = 0, \text{ otherwise,}$$

where the a priori probability $P_i = e^{-U(\phi_i)/kT}/Z$, $1/2\tau_c = D = k\delta^2/2$, δ is the unit angular step, and k is the kinetic constant associated with a unit step.

To simulate the deuterium line shape of the mobile C2′−D2″ bond for the simple one-dimensional diffusion model illustrated in Figure 8, a form for the potential U(ϕ) must be assumed. Theoretical studies of the conformational dynamics of furanose rings in DNA and RNA assume a double-well potential (*38*), with well minima closely corresponding to the C2′-endo and C3′-endo configurations of the furanose ring. A simple approximation to a double well potential has the form $U(\phi) = U_0/2(1 - \cos 2\phi)$ where the barrier height is U_0. Assuming values for U_0, the cone-half-

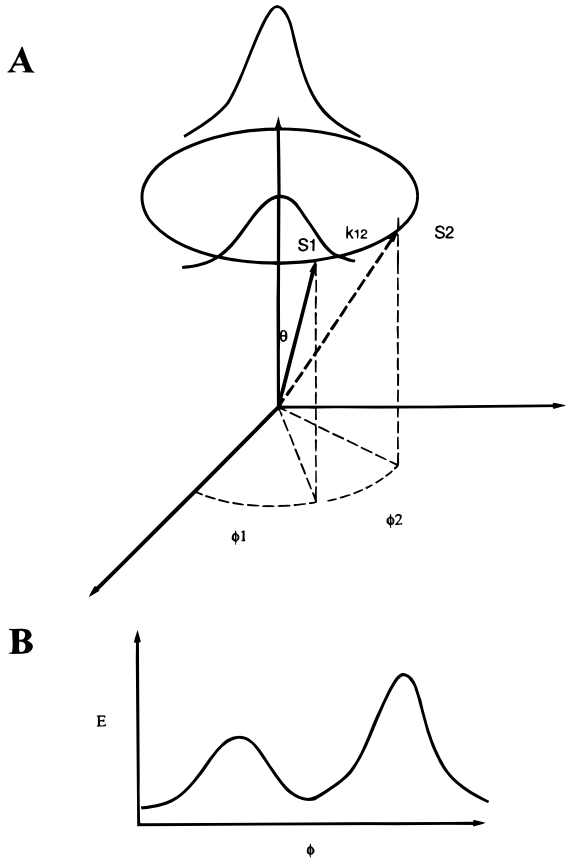

FIGURE 8: (A) Model of single axis Brownian diffusion. θ is held constant, while individual sites are designated by a value of ϕ, with a rate constant k_{ij} to distinguish the rate between sites S_i and S_j. (B) Graph showing relationship between the barrier energy and the angle ϕ. The barrier heights are shown as unequal for illustrative purposes only. The barriers with the best fits were of equal height, with the magnitudes described in the text.

angle θ (see Figure 8A), and the diffusion coefficient D, a motionally averaged deuterium line-shape can be calculated by numerical integration of

$$\dot{M}_{\pm,i} = \sum_{j=1}^{N} (i\omega_{\pm,i}\delta_{ij} + R_{ij})M_{\pm,j} \qquad (4)$$

where the complex transverse magnetization $M_{\pm} = M_{X,\pm} + iM_{Y,\pm}$. The coherence frequency ω_i is a function of the cone-half-angle θ, the angle ϕ_i and the angles (Φ, Θ) that relate the molecule-fixed frame to the lab frame i.e.

$$\omega_{\pm,i} = \pm\frac{3}{4}\frac{e^2qQ}{\hbar}\left[\frac{1}{4}(3\cos^2\theta - 1)(3\cos^2\Theta - 1) - \frac{3}{4}\sin 2\theta \sin 2\Theta \cos(\phi_i + \Phi) + \frac{3}{4}\sin^2\theta \sin^2\Theta \cos 2(\phi_i + \Phi)\right] \qquad (5)$$

and the matrix elements R_{ij} are given by eq 3 above. Simulated line-shapes for the 2″ deuteron of C_9, displayed in Figure 9 assume a barrier height $U_0 = 5\ k_BT$ ($T = 300$ K) and show a marked sensitivity to cone-half-angle θ and the coefficient of angular diffusion D. The effect of varying the barrier height U_0 from 4.5 to 6 k_BT on the deuterium line-shape is shown in Figure 10. Best fits to the experimental spectra of the 2″ deuteron of C_9 in methylated and unmethylated are shown in Figure 5, parts C and D, parts 6, C and D. All have a barrier height of 5 k_BT. Both parts of Figure 5, C and D, have a rate constant of $k = 7.5 \times 10^7$ Hz and half-angle amplitudes of 34° and 38°, respectively. Additionally, both parts of Figure 6, C and D, have rate constants of $k = 10^8$ Hz and half-angle amplitudes of 34° and 38°, respectively. These simulations show that the primary effect of methylation is to diminish the cone-half-angle from about 38° to 34° or a total reduction in the dynamic amplitude of the C2′−D2″ bond from 76° to 68°.

It is interesting to note that, while methylation affects the amplitude of sugar ring motion, the puckering rate is unaffected. The rate at which the C2′−D2″ bond passes over the barrier U_0 can also be estimated following the treatment of Edholm and Blomberg (*36*), where the "escape" rate or the rate of passage over the barrier is approximated by

$$\text{Escape rate} \approx \left[-\left[\frac{\partial^2 U}{\partial \delta^2}\right]_{\text{top}}\left[\frac{\partial^2 U}{\partial \phi^2}\right]_{\text{bottom}}\right]^{1/2} \frac{D}{2\pi k_B T} \exp\left(-\frac{U_{\text{top}}}{k_B T}\right) \qquad (6)$$

Simulations using a double 5 k_BT barrier, a rate constant $k = 7.5 \times 10^7$ Hz, and a half-angle amplitude of 38° provide an escape rate of 1.7×10^6 Hz.

Base Motions. From the data obtained from [5,6-^{2}H]-C_9 DNA, it is clear that cytosine methylation has the least perturbing effect on the motion of the base itself. The *QCC* and asymmetry parameter for [5,6-^{2}H]-C_9 in methylated DNA are virtually identical to data from [5,6-^{2}H]-C_9 in unmethylated DNA, shown in Figure 7C where the QCC_{eff} was found to be 168 kHz with an asymmetry parameter of $\eta_{\text{eff}} = 0.06$ at $W = 10.1$. The asymmetry parameter, η_{eff}, is unaffected, and the QCC_{eff} is narrowed only slightly. The spin−lattice relaxation time, $<T_{1Z}>$ is similarly unaffected. The line-shape for [5,6-^{2}H]-C_9 has been simulated previously (*14*) as a small angle (∼9°) two-site jump superimposed on the motion of the DNA helix, and this provides a reasonable physical picture of the motion of the C_9 base in methylated DNA as well. Additionally, the spin−lattice relaxation times for the D6 deuterons in methylated and unmethylated DNA are comparable (Table 1). For the [5,6-^{2}H]-C_9 at $W = 10.1$, $<T_{1Z}> = 0.1$ s, whereas for the [d_6, methyl-$^2H_4$]-$^{5Me}C_9$ sample the value of $<T_{1Z}>$ for the D6 deuteron is 0.15 s.

Comparison of Solid-state NMR Results with other Methods. The internal dynamics of the unmethylated DNA dodecamer [d(CGCGAATTCGCG)]$_2$ have been studied by a number of experimental techniques. High-resolution solution NMR (*39*, *40*), X-ray crystallography (*41*), and solid-state NMR studies (*42*−*44*) of DNA oligomers indicate that local internal motions of the bases, the sugar rings, and the phosphodiester backbone in the d(AATT) segment are minimal in amplitude. However, in a recent solid-state ^{2}H NMR study of [d(CGCGAATTCGCG)]$_2$, where C_9 has been deuterated on the base, sugar ring, and 5′-methylene group, we reported the occurrence of large amplitude motions on the 0.1 microsecond time scale for both the furanose ring and phosphodiester backbone moieties (*14*). These local motions included variations of furanose ring torsion angles by 60−70 degrees and gauche−trans isomerizations in the phosphodiester backbone at the C_9 nucleotide at hydration levels characteristic of the biologically relevant B-form.

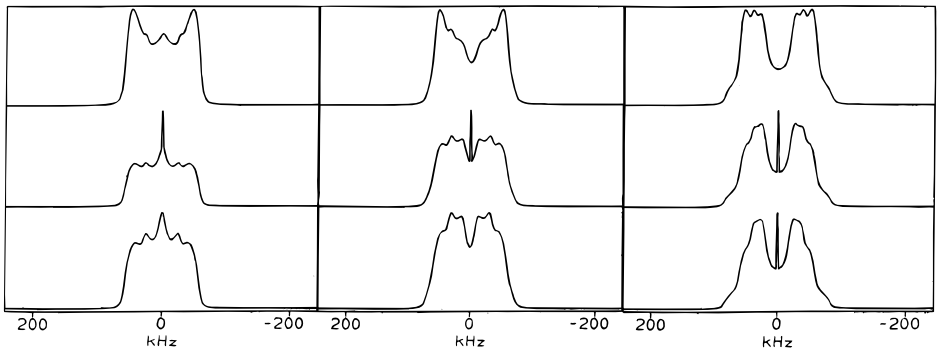

FIGURE 9: Series of simulations using the Brownian diffusion model described in the text, showing the model's dependence upon the half-angle amplitude θ and the rate constant k. All have barrier heights of 5 k_BT. The left column has a half-angle of 38°, the middle column 34°, and the right column 30°. The top row has a rate constant of $k = 5 \times 10^7$ Hz, the middle row $k = 7.5 \times 10^7$ Hz, and the bottom row $k = 1 \times 10^8$ Hz.

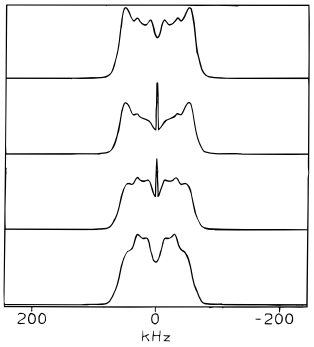

FIGURE 10: Series of simulations using the Brownian diffusion model described in the text, showing its dependence upon barrier height. All simulations have a half-angle amplitude of 34° and a rate constant of $k = 7.5 \times 10^7$ Hz. The barrier heights are (bottom to top) 4.5 k_BT, 5 k_BT, 5.5 k_BT, and 6 k_BT.

In summary, the physical picture that has emerged thus far for the internal dynamics of the *Eco*RI binding site in [d(CGCGAATT*C*GCG)]$_2$ is that amplitudes of localized motions of the phosphate−sugar backbone at the C_9 nucleotide, which is located at the AT−GC junction, are large relative to the surrounding regions, and we have demonstrated a significant reduction in the inherent mobility of the sugar−phosphate backbone at C_9 upon methylation of the cytidine base. This reduced flexibility of the C_9 backbone may result from structural modifications in the DNA (e.g., altered base stacking) caused by the substitution of an additional methyl group on the cytosine heterocycle. Inspection of X-ray coordinates for the B-DNA dodecamer, [d(CGCGAATT^{5Me}CGCG)]$_2$, indicates that both the C6−P and C6−O5′ distances of C_9 increase by approximately 0.5 Å relative to the native dodecanucleotide (*8*). However, the effects of methylation on the local structure of the DNA are not nearly as drastic as the effect on local dynamics. Because of the correlation between torsion angles in nucleic acids, it is conceivable that such subtle changes in the structure of the $^{5Me}C_9$ nucleotide could impact localized backbone motion, and it is already known that methylation of adenosine or cytosine, while not significantly altering the groove structure, does stabilize the DNA double helix as evidenced by an increase in melting temperature of the DNA (*2*, *45*, *46*).

The fact that methylation exerts its greatest influence on the dynamics of the sugar−phosphate backbone is not surprising given numerous other studies indicating the importance of the DNA backbone in DNA−protein interactions. Recent work by Mayer-Jung and co-workers indicates that partial neutralization of the negative charge of the phosphodiester backbone by cationic protein residues induces relaxation of the DNA to a bent form (*10*). A recent study of X-ray crystal structures of M.*Hha*I methyltransferase complexed with DNA substrates containing mismatches at the target site, including G:A, G:U, or G:AP (where AP = abasic site) indicate that the mismatched adenine, uracil, and abasic site are all flipped out of the DNA helix and adopt the same conformation as the normal substrate (*47*). Such data indicate that rather than the cytosine base at a CpG step being "pushed" out of the helix by the protein, the push must occur at the phosphodiester backbone. These studies indicate that local dynamics of the phosphodiester backbone, and thus its inherent flexibility, may be an important feature of protein−DNA interactions.

Conclusions. Our result that C_9 methylation quenches the large amplitude dynamics of the phosphodiester backbone coupled to the knowledge that C_9 methylation inhibits *Eco*RI binding provides strong evidence that DNA dynamics plays an important role in protein recognition and/or the cleavage mechanism in this system. The idea that interactions between proteins and DNA involve an important dynamic component is not novel. Enzyme studies suggest that the presence of both specific and nonspecific binding sites can be attributed to the rolling of the protein along the DNA and dropping into and out of different sites and binding more strongly to high affinity sites (*48*). These high affinity sites are postulated to be regions of increased DNA flexibility where the protein can kink the DNA and make the specific contacts necessary for selective binding and cleaving (*12*). This hypothesis suggests that the DNA, with internal flexibility that lowers the energy barrier for protein−DNA binding, is an active participant in the protein binding mechanism. On the other hand, the importance of DNA dynamics has been questioned by the results of X-ray studies of the *Bam*HI endonuclease (*49*, *50*). The structures of the *Bam*HI protein and the *Bam*HI/DNA complex were compared and showed significant distortions in the protein structure upon DNA binding. The DNA structure, which was only observed in the complex, was described as an undistorted B-form helix.

In summary, our work provides further support for the idea that localized dynamics of the DNA double helix may be a sequence-dependent property with a functional role. These results suggest that structural studies of protein−DNA interactions and the influence exerted on these interactions

by chemical modifications such as methylation should be coupled to dynamical investigations to fully describe how such modifications influence biological function.

ACKNOWLEDGMENT

We would like to acknowledge John Bial for assistance in operating the automated DNA synthesizer.

REFERENCES

1. Brennan, C. A., Van Cleve, M. D., and Gumport, R. I. (1986) *J. Biol. Chem. 261*, 7270−7278.
2. Adams, R. L. (1990) *Biochem. J. 265*, 309−320.
3. Ahmad, I., and Rao, D. (1996) *Crit. Rev. Biochem. Mol. Biol. 31*, 361−380.
4. Davey, C., Pennings, S., and Allan, J. (1997) *J. Mol. Biol. 267*, 276−288.
5. Coulondre, C., Miller, J. H., Farabaugh, P. J., and Gilbert, W. (1978) *Nature 274*, 775−780.
6. Ramsahoye, B. H., Davies, C. S., and Mills, K. I. (1996) *Blood Rev. 10*, 249−261.
7. Hodges-Garcia, Y., and Hagerman, P. J. (1992) *Biochemistry 31*, 7595−7599.
8. Partridge, B. L. (1996), Cambridge University.
9. Lefebvre, A., Mauffret, O., el Antri, S., Monnot, M., Lescot, E., and Fermandjian, S. (1995) *Eur. J. Biochem. 229*, 445−454.
10. Mayer-Jung, C., Moras, D., and Timsit, Y. (1997) *J. Mol. Biol. 270*, 328−335.
11. Alleman, R. K., and Egli, M. (1997) *Chem. Biol. 4*, 643−650.
12. Stryer, L. (1988) *Biochemistry*, New York.
13. McClarin, J. A., Frederick, C. A., Wang, B., Greene, P., Boyer, H. W., Grable, J., and Rosenberg, J. M. (1986) *Science 234*, 1526−1541.
14. Hatcher, M. E., Mattielo, D. L., Meints, G. A., Orban, J., and Drobny, G. P. (1998) *J. Am. Chem. Soc. 120*, 9850−9862.
15. Dickerson, R. E., and Drew, H. R. (1981) *J. Mol. Biol. 149*, 761−786.
16. Shui, X., McFail-Isom, L., Hu, G. G., and Williams, L. D. (1998) *Biochemistry 37*, 8341−8355.
17. Robins, M. J., Wilson, J. S., and Hansske, F. (1983) *J. Am. Chem. Soc. 105*, 4059−4065.
18. Orban, J., and Reid, B. R. (1989) *J. Labelled Compd. Radiopharm. 27*, 195−198.
19. Krenitsky, T. A., Rideout, J. L., Chao, E. Y., Koszaika, G. W., Gurney, F., Crouch, R. C., Cohn, N. K., Wolberg, G., and Vinegar, R. (1986) *J. Med. Chem. 29*, 138−143.
20. Cowart, M., Gibson, K. J., Allen, D. J., and Benkovic, S. J. (1989) *Biochemistry 28*, 1975−1983.
21. Weast, R. C. (1979) in *Handbook of Chemistry and Physics*, CRC Press, Boca Raton, FL.
22. Tycko, R. (1983) *Phys. Rev. Lett. 51*, 775−777.
23. deFontaine, D. L., Ross, D. L., and Ternai, B. J. (1975) *J. Mag. Reson. 18*, 276.
24. Vold, R. L., and Vold, R. R. (1991) in *Advances in Magnetic and optical Resonance* (Press, A., Ed.), San Diego.
25. Alam, T. M., and Drobny, G. P. (1991) *Chem. Rev. 91*, 1545−1590.
26. Alam, T. M., Orban, J., and Drobny, G. P. (1991) *Biochemistry 30*, 9229−9237.
27. Kilpatrick, J. E., Pitzer, K. S., and Spitzer, R. (1947) *J. Am. Chem. Soc. 69*, 2483.
28. Altona, C., and Sundaralingam, M. (1972) *J. Am. Chem. Soc. 94*, 8205−8212.
29. Levitt, M., and Warshel, A. J. (1978) *J. Am. Chem. Soc. 100*, 2697.
30. Bax, A., and Lerner, L. (1988) *J. Mag. Reson. 79*, 429−438.
31. Ulyanov, N. B., Schmitz, U., Kumar, A., and James, T. L. (1995) *Biophys. J. 68*, 13−24.
32. Olson, W. K., and Sussman, J. S. (1983) *J. Am. Chem. Soc. 104*, 270.
33. Nadler, W., and Schulten, K. (1986) *J. Chem. Phys. 84*, 4015−4025.
34. Nadler, W., and Schulten, K. (1984) *Proc. Natl. Acad. Sci. U.S.A. 81*, 5719−5723.
35. Wittebort, R. J., Olejniczak, E. T., and Griffin, R. G. (1987) *J. Chem. Phys. 86*, 5411−5420.
36. Edholm, O., and Blomberg, C. (1979) *Chem. Phys. 42*, 449−464.
37. Torchia, D. A., and Szabo, A. (1982) *J. Mag. Reson. 49*, 107−121.
38. Saenger, W. (1984) *Principles of Nucleic Acid Structure*, Springer-Verlag New York, Inc., New York.
39. Zhu, L., Reid, B. R., Kennedy, M., and Drobny, G. P. (1994) *J. Mag. Reson., Ser. A 111*, 195−202.
40. Nuutero, S., Fujimoto, B. S., Flynn, P. F., Reid, B. R., Ribiero, N. S., and Schurr, J. M. (1994) *Biopolymers 34*, 463−480.
41. Holbrook, S. R., and Kim, S.-H. (1984) *J. Mol. Biol. 173*, 361−388.
42. Huang, W.-C., Orban, J., Kintanar, A., Reid, B. R., and Drobny, G. P. (1990) *J. Am. Chem. Soc. 112*, 9059−9068.
43. Kintanar, A., Alam, T. M., Huang, W.-C., Schindele, D. C., Wemmer, D. E., and Drobny, G. P. (1988) *J. Am. Chem. Soc. 110*, 6367.
44. Alam, T. M., and Drobny, G. P. (1990) *Biochemistry 29*, 3421−3430.
45. Frederick, C. A., Quigley, G. L., van der Marel, G. A., van Boom, J. H., Wang, A. H., and Rich, A. (1988) *J. Biol. Chem. 263*, 17872−17879.
46. Collins, M., and Myers, R. M. (1987) *J. Mol. Biol. 198*, 737−744.
47. O'gara, M., Horton, J. R., Roberts, R. J., and Cheng, X. (1998) *Nat. Struct. Biol. 5*, 872−877.
48. Lesser, D. R., Kurpiewski, M. R., and Jen-Jacobson, L. (1990) *Science 250*, 776−786.
49. Newman, M., Strzelecka, T., Dorner, L. F., Schildkraut, I., and Aggwarl, A. K. (1994) *Nature 368*, 660−664.
50. Newman, M., Strzelecka, T., Dorner, L. F., Schildkraut, I., and Aggarwal, A. K. (1995) *Science 269*, 656−663.

BI9917636